Dalton Transactions

Direct Electrospinning of Titania Nanofibers with Ethanol

Journal:	*Dalton Transactions*
Manuscript ID	DT-COM-05-2019-001872.R1
Article Type:	Communication
Date Submitted by the Author:	22-Jul-2019
Complete List of Authors:	Chapman, Brian; North Carolina State University Mishra, Sumeet; North Carolina State University, Department of Materials Science and Engineering Tracy, Joseph; North Carolina State University, Department of Materials Science and Engineering

Dalton Transactions

COMMUNICATION

Direct Electrospinning of Titania Nanofibers with Ethanol

Brian S. Chapman, Sumeet R. Mishra and Joseph B. Tracy*

Received 00th January 20xx,
Accepted 00th January 20xx

DOI: 10.1039/x0xx00000x

www.rsc.org/

Titanium(IV) isopropoxide in ethanol is aged under acidic conditions with a small amount of water. After adding a small amount of *N*,*N*-dimethylformamide, TiO_2 nanofibers with average diameters of ~70 nm are prepared by direct electrospinning. During *in situ* heating of the nanofibers, crystallization into anatase and rutile phases is observed.

Introduction

Nanoscale ceramic fibers are of interest for their high surface-area-to-volume ratio and have widespread applications, including electronics, sensors, and catalysis.[1,2] Anatase titania (TiO_2), in particular, is a promising photocatalyst for water splitting, environmental remediation, and nanomedicine.[3-6] It is also appealing to combine TiO_2 nanostructures with inorganic nanoparticles for modifying their phototcatalytic behaviour or incorporating additional functionality.[7-11] Here, we report electrospinning of TiO_2 nanofibers with average diameters below 100 nm and without use of a polymer additive. To the best of our knowledge, this is the smallest diameter of direct electrospun TiO_2 fibers obtained to date, where the smallest diameter previously reported is 510 nm.[12] This work builds upon previous studies of direct electrospun TiO_2 fibers,[12,13] which required use of a toxic solvent, 2-methoxyethanol.[14-16] In this work, ethanol is a more environmentally friendly substitute, though we also use a small amount (<5 v%) of *N*,*N*-dimethylformamide (DMF) to facilitate electrospinning.

Electrospinning is an established method for producing ceramic fibers with sub-µm diameters and lengths exceeding 100 µm.[1] In electrospinning, a high-voltage power supply is connected to a solution reservoir, usually a syringe, and a grounded deposition plate. As the solution is slowly pumped through the syringe under the applied voltage, instead of forming a bead at the tip of the needle, the solution stretches and elongates into a "Taylor cone." When the Coulomb force exerted on the Taylor cone is high enough to overcome the surface tension of the solution, a stream of polymer solution jets from the tip of the cone. As the jet of polymer solution travels through the air, the solvent evaporates, and a fiber forms, which is whipped and stretched through the air by the applied electric field. Numerous polymers have been electrospun into fibers.[17]

Two approaches have been developed for fabricating ceramic fibers by electrospinning, a polymer-assisted method and a method that uses only sol-gel chemistry. In polymer-assisted electrospinning, a ceramic precursor, often a sol, a salt, or nanoparticles, is mixed with a polymer solution.[18] The polymer controls the electrospinning process and provides the appropriate rheology for electrospinning. Electrospun fibers are then calcined at temperatures above 450 °C to simultaneously remove the polymer additive and sinter the ceramic precursors. The disadvantage of this approach is that the samples can undergo significant shrinkage, which can result in breakage of the fibers and can be especially problematic when fibers are deposited directly onto a support material.[1] Polymer additives can also leave carbon residues in the fibers.[19] Because the polymer guides the electrospinning process, many types of ceramic fibers have been synthesized through this polymer-assisted approach,[20] including TiO_2,[21,22] $BaTiO_3$,[23] $BaTiO_3/CoFe_2O_4$,[24] Al_2O_3,[25] SiO_2,[26] $NiFe_2O_4$,[27] SiC,[28] B_4C,[29] and $C/Ge/GeO_2$.[30]

In direct electrospinning, no organic polymer is added, and the solution prepared for electrospinning must have suitable rheology.[31] By mixing the alkoxide precursor, solvent, water, and an acid, conditions can be obtained that allow for electrospinning without adding a polymer. While direct electrospinning avoids the need for calcination and the associated challenges discussed above, obtaining a sol with the appropriate viscosity for electrospinning can be challenging. Because of this issue, there have been only a few reports of

[a] Department of Materials Science and Engineering, North Carolina State University, Raleigh, North Carolina 27695, USA. E-mail: jbtracy@ncsu.edu.
†Electronic Supplementary Information (ESI) available: SEM images of TiO_2 fibers and particles obtained when varying the conditions for electrospinning. See DOI: 10.1039/x0xx00000x

direct electrospun ceramic fibers composed of SiO_2,[32-34] Al_2O_3,[35] $PbZrTiO_2$,[36,37] and TiO_2.[12,13] Another drawback of direct electrospinning is that the fiber diameters are generally greater than 1 μm, with one exception, where TiO_2 fibers of 500 nm were produced.[12] As noted earlier, an issue specific to direct electrospinning of TiO_2[12,13] is the use 2-methoxyethanol,[14-16] a known teratogen and mutagen.

For direct electrospinning, hydrolysis and condensation of the alkoxide precursor need to be controlled to yield a network of long chains with minimal crosslinking or branching, allowing for maximum entanglement and minimal gelation during electrospinning.[34,38] The following steps can provide the necessary control: An acid rather than base should be used to catalyze condensation. Acid catalysis drives formation of linear, ladder-like structures, allowing for the formation of viscous sols before gelation. In contrast, base catalysis causes branching and more readily produces nanoparticles, which does not allow for facile control of the viscosity.[38] The composition of the mixture is also important, and a molar ratio of 2 water : 1 alkoxide typically forms a sol with the ideal morphology.[35] Reducing the concentration can minimize crosslinking and favors electrospinning, while electrospinning of more highly concentrated sols is inhibited.[34]

Previous reports on electrospinning TiO_2 fibers either used polymer additives to assist electrospinning and required calcination or, for direct electrospinning, yielded large fiber diameters (> 500 nm) and used a toxic solvent.[12,13] Here, we report use of ethanol-based sols for direct electrospinning of TiO_2 nanofibers without use of polymer additives and with average diameters below 100 nm, which is also the first example of direct-electrospun ceramic fibers with diameters below 100 nm.

Experimental Section

Sol Gel Synthesis

Titanium(IV) isopropoxide (TTIP, Acros Organics, 98%), anhydrous ethanol (Sigma-Aldrich, 99.5%), HNO_3 (Sigma-Aldrich, 70%), and DMF (EMD, OmniSolv, 99.99%) were used to prepare a sol for electrospinning TiO_2 fibers. The sol was developed by modifying a previous method for direct electrospinning of TiO_2 fibers,[13] and 2-methoxyethanol was replaced with ethanol. 25 mL of ethanol was added to a 40-mL vial with a septum cap inside a glove box, to which 1.42 g of TTIP was added dropwise with rapid stirring and allowing complete mixing of the solution between drops. The vial was then sealed, magnetically stirred for 10 minutes, and removed from the glove box. 15.5 μL of concentrated HNO_3 was then injected through the septum, and the vial was stirred for another 10 minutes. The vial was then opened to the air and heated at 80 °C for 90 minutes with moderate stirring, followed by cooling to room temperature and rotary evaporation to reduce the volume of the sol to ~1 mL. 50 μL of DMF was then added, followed by stirring for 10 minutes. The sol was loaded into a 3-mL syringe and capped. If not used immediately, the electrospinning solution was stored in the capped syringe in a freezer at -16 °C. After 2 months of storage, the solution showed no signs of gelation and remained suitable for electrospinning.

The combination of partially completing the condensation reaction and rotatory evaporation to control the viscosity of sol make precise reproducibility of the sol from one preparation to the next challenging. An additional variable may be the effect of variations in environmental humidity, because the sol is prepared using only a small amount of water (in the concentrated HNO_3). In general, variations among different batches of the sol can be compensated by adjusting the electrospinning conditions. If the syringe with the sol is capped and stored in the freezer, the same set of parameters can be used for electrospinning on different days, which suggests the electrospinning process is relatively insensitive to the environmental humidity.

Electrospinning

A home-built setup was used for electrospinning, consisting of a vented enclosure, horizontally oriented syringe pump, syringe, blunt-tipped needle, grounded collector plate covered with Al foil, and 30 kV power supply (Bertan Associates, Inc, 205A-30P). The syringe prepared as described above was fitted with a 22-gauge, 1.5”-long, blunt-tipped needle. After pushing any air bubbles and a small amount of the solution out of the syringe, it was loaded in the syringe pump, and the metal needle was connected to the positive terminal of the power supply with an alligator clip. The ground terminal was connected to the collector plate. Using a tip-collector distance of 14 cm, the flow rate was set 1.0 μL/min, and the voltage was set to 14 kV. After stopping electrospinning, 10 minutes elapsed before opening the enclosure and removing the sample, both to allow any residual charges on the needle and collector to dissipate, and to purge the enclosure of any TiO_2 fibers that were not anchored to the collector or other surfaces. After removing the sample, all surfaces inside the enclosure were wiped down with a damp cloth to remove any fibers that did not deposit on the plate. (Caution: The high voltage poses an electrocution hazard, and electrospinning should only be conducted with appropriate training. Enclosing the electrospinning setup in a box with interlocks can reduce the potential for exposure to the high voltage. TiO_2 fibers also become airborne easily and pose an inhalation hazard.)

Because of the limitations noted above in precisely controlling the extent on condensation and viscosity of the sol, the parameters for electrospinning may need to be adjusted to account for variations among different batches. The correct parameters were found by first adjusting the flow rate until fibers started forming, followed by adjusting the voltage and tip-collector distance until continuous fibers formed. The presence of fibers was verified by depositing a test sample onto a small square of Al foil and viewing it on an optical microscope. As an example, SEM images of the products of electrospray and electrospinning obtained at different applied voltages and tip-collector distances are presented in the ESI, Fig. S1.† Those results were obtained from a different sol and at a different flow rate, which gave a different optimal voltage for electrospinning.

We did not notice a significant dependence of the fiber diameter on the flow rate.

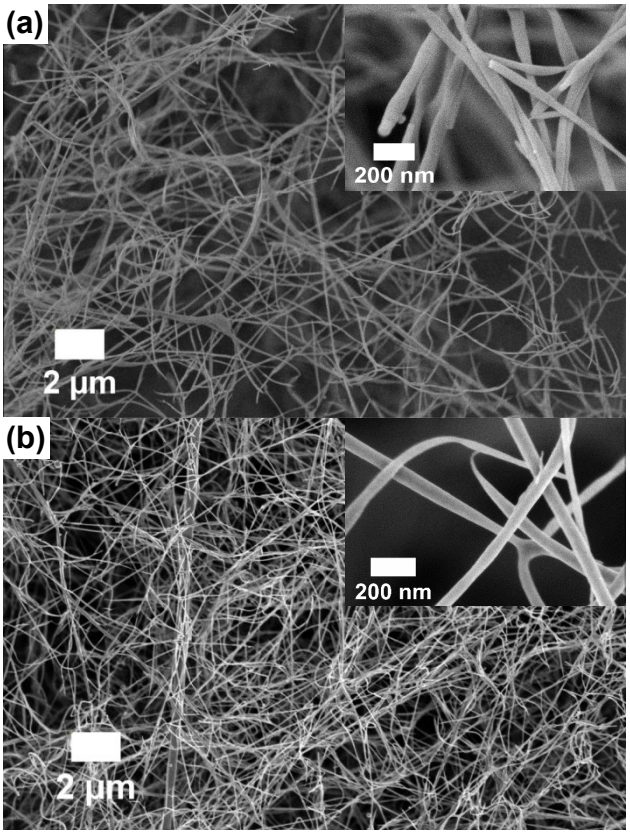

Figure 1. SEM images of amorphous TiO_2 nanofibers on a Si wafer (a) prior to heating and (b) after heating to 450 °C in air for 2 hours. Insets show the samples at higher magnification.

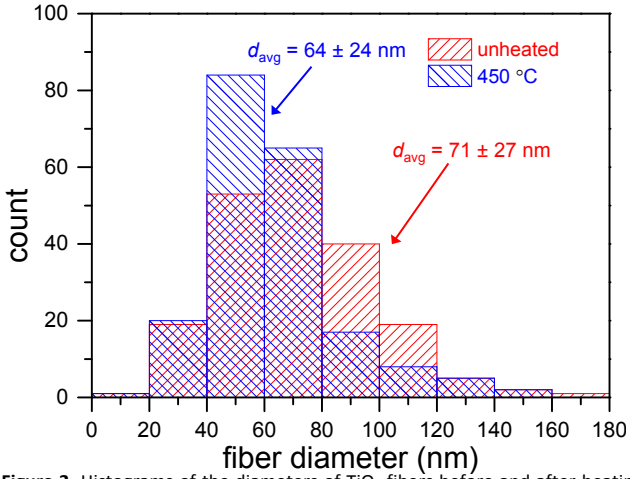

Figure 2. Histograms of the diameters of TiO_2 fibers before and after heating to 450 °C in air for 2 hours. For each sample, 200 fibers were measured.

Characterization and Conversion into Anatase TiO_2

The fibers were imaged by scanning electron microscopy (FEI Verios 460L). For *in situ* X-ray diffraction (XRD) measurements, samples were collected on Si wafers affixed to the Al foil with double-sided tape. The samples were loaded into a X-Ray diffractometer (PANalytical Empyrean) with a heating stage (XRK 900) and heated under ambient atmosphere to 900 °C at a rate of 1 °C/min. Diffractograms were collected continuously, and each diffractogram had a ~15 minute acquisition time. 2θ was scanned from 20° to 45° in steps of 0.026°.

Results and Discussion

Fiber Morphology

Nanoscale amorphous TiO_2 fibers were direct electrospun (Figure 1a) without using an organic polymer to assist electrospinning. The fibers do not exhibit beading or crosslinking between fibers, which are common challenges in electrospinning. The as-spun fibers have an average diameter of 71 ± 27 nm (Figure 2). This multifold decrease in fiber diameter, based on comparison with previous studies,[12,13] can be partially attributed to replacing 2-methoxyethanol with ethanol. Using solvents with a higher vapor pressure has been shown to decrease the diameter of polymeric nanofibers.[39] Using slower flow rates than are commonly employed for direct electrospinning may also contribute to the decreased fiber diameter.[40]

A sample of TiO_2 fibers was heated to 450 °C for two hours (Figure 1b), which mimics conditions for calcining fibers that contain organic polymers.[21] The morphology of the fibers is maintained and there are no signs of breakage. The average fiber diameter after calcining is 64 ± 24 nm. This 10% decrease in diameter can be attributed to generation and evaporation of ethanol as condensation is completed, yielding pure TiO_2 fibers.

Guidance for Preparing the TiO_2 Sol

The following guidance is based on the more extensive literature for direct electrospinning of SiO_2 fibers.[32-34] The key to direct electrospinning of SiO_2 fibers without polymer additives is producing a sol where the gel forms long chains and minimizes branching or crosslinking. Excessive branching could inhibit electrospinning and result instead in electrospray. Lowering the pH of the solution minimizes branching, because acid-catalyzed reactions preferentially form chains. The water content and temperature are also important for controlling the rate of crosslinking, even though TTIP is less reactive than many other titanium alkoxides. For this reason, it is important to use anhydrous ethanol. If condensation occurs too quickly, precipitates will form and inhibit fiber formation. Precipitation in the sol is indicated by the appearance of cloudiness. Water needs to be introduced in a controlled manner to keep the reaction slow enough that long chains form. The 2:1 ratio of alkoxide to water recommended in the literature drove condensation too quickly and caused formation of precipitates in the sol. In order to avoid formation of precipitates, the only water introduced into the system is from the concentrated HNO_3 and ambient humidity. Crosslinking is further minimized by performing the reaction under dilute conditions. In preparation for electrospinning, rotary evaporation was used to reduce the volume to 1 mL, yielding a sol with appropriate viscosity for electrospinning. The rheology of the sol was not measured because of its corrosive nature and the potential to damage the plates of the rheometer.

Guidance for Electrospinning

Several parameters are important for obtaining contiguous TiO_2 fibers with uniform diameters. The tip-collector distance is especially important. As the distance between the tip of the needle and the collector plate increases, the rate of deposition and number of TiO_2 particles present in the sample decrease. It is unclear if the particles no longer form under these conditions, or if they do not deposit onto the collector plate. Higher than optimal voltages appear to produce thin fragments of fibers, along with particles. At higher voltages, instability in the fibers due to their narrow diameter and weak entanglement in the TiO_2 sol may result in breakage into spherical particles. Minor changes in the flow rate can also result instead in electrospray or short TiO_2 fibers.

Challenges unique to direct electrospinning of oxide fibers include the presence of short fibers and nanoparticles. Polymer entanglement, which is controlled by the polymer chain length and molecular weight, is critically important for electrospinning. The polymer chains in a TiO_2 sol are shorter than for polymer solutions commonly employed for electrospinning polymers. As a result, direct electrospinning of TiO_2 can be more challenging than polymer-assisted electrospinning. The short chains in TiO_2 sols limit the extent of entanglement, and suboptimal conditions for electrospinning can yield particles or short segments of fibers instead of contiguous fibers.

When attempting direct electrospinning of TiO_2 fibers from a purely ethanol-based sol, only electrospray was achieved, and some of the solution crystalized at the tip of the needle. Including a small amount of DMF, which has a high boiling point, in the sol facilitates electrospinning by slowing evaporation of the solvent and inhibiting crystallization of TiO_2.[41]

In Situ X-Ray Diffraction

Formation of the anatase phase, followed by the rutile phase, was monitored by *in situ* XRD measurements of the TiO_2 fibers during heating to 900 °C under ambient atmosphere. Diffractograms were acquired at intervals of ~15 °C for 2θ between 20° and 45°, which contains the most prominent peaks for the anatase and the rutile phases (Figure 3). The intensity of the broad background from amorphous TiO_2 decreases as the temperature approaches 500 °C. The anatase (101) peak appears by 496 °C, and the anatase (004) peak emerges by 743 °C. The rutile (110) peak appears by 867 °C.

In comparison, in previous work on direct-electrospun TiO_2 fibers with a diameter of ~2 µm, the anatase and rutile phases formed at 250 °C and 600 °C, respectively.[13] Comparable polymer-assisted electrospun TiO_2 fibers reported the emergence of anatase peaks at 450-550 °C, with rutile appearing at 575-700 °C.[42-44] For TiO_2 powders and films that were analysed using a similar *in situ* method, anatase and rutile peaks appear at 400-500 °C and 600-850 °C, respectively.[45,46] Our observed conversion temperature for the anatase phase is consistent with these previous studies, while rutile was not observed until reaching 890 °C. Elevation of the rutile phase transition temperature is consistent with other studies of nanoscale TiO_2.[33,45,47] For *in situ* measurements, higher phase transition temperatures are also expected, if the heating rate is too fast to allow equilibration at each temperature.

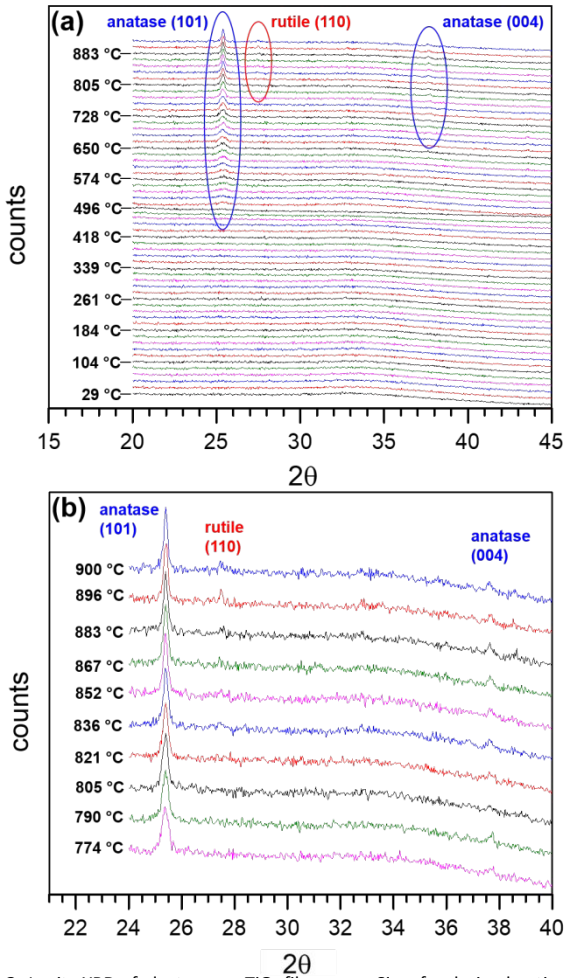

Figure 3. *In situ* XRD of electrospun TiO_2 fibers on a Si wafer during heating in air to 900 °C at a rate of 1 °C / min. Diffractograms were acquired simultaneously with heating, and each scan took ~15 minutes. The temperature labels indicate the temperature at the end of each scan. (a) All measurements and (b) the same measurements plotted between 774 and 900 °C and over a narrower range of 2θ to highlight peaks emerging at higher temperatures.

Conclusions

These results highlight the viability of direct electrospinning of TiO_2 nanofibers by using sol gel chemistry to adjust the viscosity of the sol and by modifying the parameters for electrospinning, most notably a slower flow rate than is often used. These conditions also result in a smaller fiber diameter than is typical for direct-electrospun ceramic fibers. Eliminating the polymer additive reduces the extent of shrinkage and breakage of the TiO_2 nanofibers during subsequent heating. Since sol gel chemistry is highly versatile and encompasses many metal oxides, this approach for direct electrospinning could likely be extended to other metal oxides or to mixed metal oxides. The solution conditions and parameters for electrospinning would need to be tailored for different precursor chemistries.

Acknowledgements

This research was supported by the National Science Foundation (DMR-1056653 and the Research Triangle MRSEC, DMR-1121107). We gratefully acknowledge Ching-Chang Chung for performing temperature-dependent XRD measurements of TiO_2 fibers, Roger Russell for advice about safe handling of TiO_2 fibers, and Jerome Cuomo for use of the power supply. This work was performed in part at the Analytical Instrumentation Facility (AIF) at North Carolina State University, which is supported by the State of North Carolina and the National Science Foundation (ECCS-1542015). The AIF is a member of the North Carolina Research Triangle Nanotechnology Network (RTNN), a site in the National Nanotechnology Coordinated Infrastructure (NNCI).

References

1 H. Wu, W. Pan, D. Lin and H. Li, *J. Adv. Ceram*, 2012, **1**, 2-23.
2 W. E. Teo and S. Ramakrishna, *Nanotechnology*, 2006, **17**, R89-R106.
3 T. Sugimoto, X. Zhou and A. Muramatsu, *J. Colloid Interface Sci.*, 2003, **259**, 43-52.
4 R. Zhang, A. A. Elzatahry, S. S. Al-Deyab and D. Zhao, *Nano Today*, 2012, **7**, 344-366.
5 J. B. Joo, M. Dahl, N. Li, F. Zaera and Y. Yin, *Energy Environ. Sci.*, 2013, **6**, 2082-2092.
6 F. U. Rehman, C. Zhao, H. Jiang and X. Wang, *Biomater. Sci.*, 2016, **4**, 40-54.
7 Y. Liao, Y. Xu and Y. Chan, *Phys. Chem. Chem. Phys.*, 2013, **15**, 13694-13704.
8 I. Fratoddi, A. Macagnano, C. Battocchio, E. Zampetti, I. Venditti, M. V. Russo and A. Bearzotti, *Nanoscale*, 2014, **6**, 9177-9184.
9 M. Dahl, Y. Liu and Y. Yin, *Chem. Rev.*, 2014, **114**, 9853-9889.
10 M.-S. Wong, C.-W. Chen, C.-C. Hsieh, S.-C. Hung, D.-S. Sun and H.-H. Chang, *Sci. Rep.*, 2015, **5**, 11978.
11 U. F. Gunputh, H. Le, R. D. Handy and C. Tredwin, *Mater. Sci. Eng., C*, 2018, **91**, 638-644.
12 Y. B. Kim, D. Cho and W. H. Park, *Mater. Lett.*, 2010, **64**, 189-191.
13 W. K. Son, D. Cho and W. H. Park, *Nanotechnology*, 2006, **17**, 439-443.
14 K. Nagano, E. Nakayama, H. Oobayashi, T. Nishizawa, H. Okuda and K. Yamazaki, *Environ. Health Perspect.*, 1984, **57**, 75-84.
15 R. R. Miller, J. A. Ayres, L. L. Calhoun, J. T. Young and M. J. McKenna, *Toxicol. Appl. Pharmacol.*, 1981, **61**, 368-377.
16 H. Ma, J. An, A. W. Hsie and W. W. Au, *Mutat. Res.*, 1993, **298**, 219-225.
17 D. Li and Y. Xia, *Adv. Mater.*, 2004, **16**, 1151-1170.
18 W. Sigmund, J. Yuh, H. Park, V. Maneeratana, G. Pyrgiotakis, A. Daga, J. Taylor and J. C. Nino, *J. Am. Ceram. Soc.*, 2006, **89**, 395-407.
19 R. W. Tuttle, A. Chowdury, E. T. Bender, R. D. Ramsier, J. L. Rapp and M. P. Espe, *Appl. Surf. Sci.*, 2008, **254**, 4925-4929.
20 X. Lu, C. Wang, F. Favier and N. Pinna, *Adv. Energy Mater.*, 2017, **7**, 1601301.
21 D. Li and Y. Xia, *Nano Lett.*, 2003, **3**, 555-560.
22 C. Tekmen, A. Suslu and U. Cocen, *Mater. Lett.*, 2008, **62**, 4470-4472.
23 J. Yuh, J. C. Nino and W. M. Sigmund, *Mater. Lett.*, 2005, **59**, 3645-3647.
24 J. D. Starr, M. A. K. Budi and J. S. Andrew, *J. Am. Ceram. Soc.*, 2015, **98**, 12-19.
25 A.-M. Azad, *Mater. Sci. Eng., A*, 2006, **435**, 468-473.
26 C. Shao, H. Kim, J. Gong and D. Lee, *Nanotechnology*, 2002, **13**, 635-637.
27 D. Li, T. Herricks and Y. Xia, *Appl. Phys. Lett.*, 2003, **83**, 4586-4588.
28 H. A. Liu and K. J. Balkus, *Mater. Lett.*, 2009, **63**, 2361-2364.
29 D. T. Welna, J. D. Bender, X. Wei, L. G. Sneddon and H. R. Allcock, *Adv. Mater.*, 2005, **17**, 859-862.
30 F. Pantò, Y. Fan, S. Stelitano, E. Fazio, S. Patanè, P. Frontera, P. Antonucci, N. Pinna and S. Santangelo, *Adv. Funct. Mater.*, **28**, 1800938.
31 P. S. Kumar, S. Jayaraman and G. Singh, in *Rheology and Processing of Polymer Nanocomposites*, eds. S. Thomas, R. Muller and J. Abraham, Wiley, 2016, ch. 9, pp. 329-354.
32 S.-S. Choi, S. G. Lee, S. S. Im, S. H. Kim and Y. L. Joo, *J. Mater. Sci. Lett.*, 2003, **22**, 891-893.
33 G. Zhang, W. Kataphinan, R. Teye-Mensah, P. Katta, L. Khatri, E. A. Evans, G. G. Chase, R. D. Ramsier and D. H. Reneker, *Mater. Sci. Eng., B*, 2005, **116**, 353-358.
34 J. Geltmeyer, L. Van der Schueren, F. Goethals, K. De Buysser and K. De Clerck, *J. Sol-Gel Sci. Technol.*, 2013, **67**, 188-195.
35 V. Maneeratana and W. M. Sigmund, *Chem. Eng. J.*, 2008, **137**, 137-143.
36 W. Yu and J. S.-A. Jorge, *Nanotechnology*, 2004, **15**, 32-36.
37 Y. Wang and J. J. Santiago-Avilés, *Integr. Ferroelectr.*, 2011, **126**, 60-76.
38 S. Sakka and T. Yoko, *J. Non-Cryst. Solids*, 1992, **147**, 394-403.
39 A. S. Asran, M. Salama, C. Popescu and G. H. Michler, *Macromol. Symp.*, 2010, **294**, 153-161.
40 J. Y. Park, I. H. Lee and G. N. Bea, *J. Ind. Eng. Chem.*, 2008, **14**, 707-713.
41 L. Du, H. Xu, Y. Zhang and F. Zou, *Fiber Polym.*, 2016, **17**, 751-759.
42 H. Vasquez, H. Gutierrez, K. Lozano and G. Leal, *J. Eng. Fiber. Fabr.*, 2015, **10**, 129-136.
43 A. Kumar, R. Jose, K. Fujihara, J. Wang and S. Ramakrishna, *Chem. Mater.*, 2007, **19**, 6536-6542.
44 B. Caratão, E. Carneiro, P. Sá, B. Almeida and S. Carvalho, *J. Nanotechnol.*, 2014, **2014**, 472132.
45 S. Patra, C. Davoisne, H. Bouyanfif, D. Foix and F. Sauvage, *Sci. Rep.*, 2015, **5**, 10928.
46 H. M. Albetran, B. H. O'Connor and I. M. Low, *J. Am. Ceram. Soc.*, 2017, **100**, 3199-3207.
47 H. Zhang and J. F. Banfield, *J. Mater. Chem.*, 1998, **8**, 2073-2076.

Table of Contents Entry

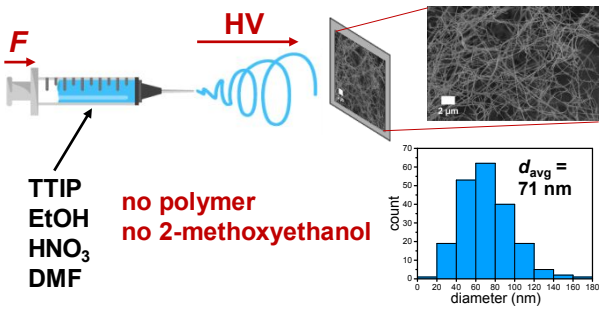

TiO_2 nanofibers with average diameters of ~70 nm were prepared by direct electrospinning.